

Spectral lags caused by the curvature effect of fireballs

R.-J. Lu^{1,2,3,4}, Y.-P. Qin^{1,2}, Z.-B. Zhang^{1,3}, T.-F. Yi²

¹*National Astronomical Observatories/Yunnan Observatory, Chinese Academy of Sciences,
P. O. Box 110, Kunming 650011, China*

²*Physics Department, Guangxi University, Nanning, Guangxi 530004, P. R. China*

³*The Graduate School of the Chinese Academy of Sciences;*

⁴*E-mail:luruijing@126.com*

Accepted ??. Received ??.; in original form 2005 June 10

ABSTRACT

Recently, Shen et al. (2005) studied the contributions of curvature effect of fireballs to the spectral lag and showed that the observed lags could be accounted for by the effect. Here we check their results by performing a more precise calculation with both the formulas presented in Shen et al. (2005) and Qin et al. (2004). Several other aspects which were not considered in Shen et al. (2005) are investigated. We find that in the case of ultra-relativistic motions, both formulas are identical as long as the whole fireball surface is concerned. In our analysis, the previous conclusion that the detected spectral lags could be accounted for by the curvature effect is confirmed, while the conclusion that the lag has no dependence on the radius of fireballs is not true. We find that introducing extreme physical parameters is not the only outlet to explain those observed large lags. Even for the larger lags ($\sim 5s$) (see Norris et al. 2005), a wider local pulse ($\Delta t_{\theta,FWHM} = 10^7s$) could account for it. Some conclusions not presented in Shen et al. (2005) or those modified in our analysis are listed below: a) lag $\propto \Gamma^{-\epsilon}$ with $\epsilon > 2$; b) lag is proportional to the local pulse width and the $FWHM$ of the observed light curves; c) a large lag requires a large α_0 and a small β_0 as well as a large E_{0p} ; d) when the rest frame spectrum varies with time, the lag would become larger; e) lag decreases with the increasing of R_c ; f) lag $\propto E$ within the certain energy range for a given Lorentz factor; g) lag is proportional to the opening angle of uniform jets when $\theta_j < 0.6\Gamma^{-1}$.

Key words: relativity – gamma-rays: bursts –gamma-rays: theory.

1 INTRODUCTION

It is common that there is a spectral lag between different energy channels in gamma-ray bursts (see, e.g. Cheng et al. 1995; Norris et al. 1996, 2000; Wu & Fenimore 2000; Chen et al. 2005). Although There are several attempts to explain the origin of the spectral lag (See, e.g., Salmonson 2000; Ioka & Nakamura 2001; Schaefer 2004; Kocevski et al. 2003a), the problem remain unresolved.

Recently, Shen et al. (2005) (hereafter Paper I) tentatively studied the contribution of curvature effect of fireball to the lag, and the resulting lags are very closed to the observed one. In fact, in their paper introducing extreme physical parameters such as $\Gamma < 50$ or $\alpha > -0.5$ is not the only outlet to explain those observed large lags. A reasonable intrinsic pulse width t'_d , i.e., hundreds to thousands of seconds, which could produce the lag of $0.1 - 1$ s based on their model, could also account for it.

Qin (2002) had derived in a much detail the flux intensity based on the model of highly symmetric expanding fireballs, where the Doppler effect of the expanding fireball surface is the key factor to be concerned, and no terms are omitted in his derivation, therefore the formula is applicable to the cases of relativistic, sub-relativistic, and non-relativistic motions and to those of spherical fireballs or uniform jets. With this formula, Qin (2003, 2004) derived the observed photon count rate of a fireball (See Eq. (1) in the paper).

A detailed comparison between Shen et al. (2005) and Qin et al. (2004) model (hereafter Paper II) gives rise to the conclusion that the two models are identical when the following conditions are satisfied. Firstly, as shown in equation (8) of Paper II, the two quantities, local time t_θ and observed time t , are related by $t = (1 - \beta \cos\theta)(t_\theta - t_c) + t_c + D/c - R_c \cos\theta/c$, where t_c is the initial local time, R_c is the radius of the fireball measured at $t_\theta = t_c$, and D is the distance of the fireball to the observer. When taking $t_c = 0$ and $T = t + (R_c - D)/c$, one would find that the above relation will become the one determined by equation (3) in Paper I (where T is referred to as observed time defined in Paper I). Secondly, in equation (3) of Paper II, the integral lower and upper limit are determined by $\tilde{\theta}_{\min} = \cos^{-1} \min\{\cos\theta_{\min}, (t_{\theta,\max} - t + D/c)/((t_{\theta,\max} - t_c)\beta + R_c/c)\}$ and $\tilde{\theta}_{\max} = \cos^{-1} \max\{\cos\theta_{\max}, (t_{\theta,\min} - t + D/c)/((t_{\theta,\min} - t_c)\beta + R_c/c)\}$, respectively, where θ_{\min} and θ_{\max} are confined by the concerned area of the fireball surface, and $t_{\theta,\min}$ and $t_{\theta,\max}$ are confined by the local time range of emission. For such a local pulse, $t_{\theta,\min} = 0$ and $t_{\theta,\max} \rightarrow \infty$, when taking $\theta_{\min} = 0$ and $\theta_{\max} = \pi/2$ (i.e., the photons reaching the observer come from the whole surface of the fireball), one would

obtain $\tilde{\theta}_{\min} = 0$ and $\tilde{\theta}_{\max} = \cos^{-1}(1 - T/\tau)$ (where $\tau = R_c/c$), which are consistent with the integral lower and upper limit in equation (4) of Paper I, respectively. In a word, the mainly difference between the two models is that, Shen et al. neglected the constraint of the local pulse and the concerned area of fireball surface on the integral lower and upper limit of the observed flux (see equation (4) in their paper), which plays a important role in producing the observed light curves. Strictly, when dealing with uniform jets with a small opening angle such as $\theta < 1/\Gamma$, the formula presented in Shen et al. (2005) would fail to be applied.

We in this paper check their results by performing a more precise calculation with the two models, at the same time, several other aspects which were not considered in Shen et al. (2005) are investigated, such as lag's dependence on energy and opening angle (in Section 2). The previous conclusion that the observed spectral lags could be accounted for by the curvature effect is confirmed and some new results are obtained. For example, lag decreases with the increase of radius of fireball other than weakly dependent on it. Lag $\propto \Gamma^{-\epsilon}$, $\epsilon > 2$ in the case of fixing the local pulse width, which is identical with that, lag $\propto \Gamma^{-1}$ in the case of fixing the intrinsic pulse width, obtained by Shen et al. (2005). Accordingly an interesting question arises: would the two approaches always lead to identical results? which will be discussed in Section 3. And then we give our discussions and conclusions in the last section.

2 THEORETICAL ANALYSIS ON SPECTRAL LAGS

Under the assumption that a fireball expands isotropically with a constant Lorentz factor $\Gamma > 1$ and the radiation is independent of direction, the expected count rate of the fireball measured within frequency interval $[\nu_1, \nu_2]$ can be calculated with equation (21) in paper II, which can be rewritten as follows

$$C(\tau) = \frac{2\pi R_c^3 \int_{\tilde{\tau}_{\theta,\min}}^{\tilde{\tau}_{\theta,\max}} \tilde{I}(\tau_\theta) (1 + \beta \tau_\theta)^2 (1 - \tau + \tau_\theta) d\tau_\theta \int_{\nu_1}^{\nu_2} \frac{g_{0,\nu}(\nu_0, \theta)}{\nu} d\nu}{hcD^2 \Gamma^3 (1 - \beta)^2 (1 + \frac{\beta}{1 - \beta} \tau)^2}. \quad (1)$$

Note that the formula is in terms of the integral of τ_θ , which is a dimensionless relative local time defined by $\tau_\theta \equiv c(t_\theta - t_c)/R_c$, where t_θ is the emission time in the observer frame, called local time, of photons emitted from the concerned differential surface ds_θ of the fireball (θ is the angle to the line of sight), t_c is the initial local time which could be assigned to any values of t_θ , and R_c is the radius of the fireball measured at $t_\theta = t_c$. Variable τ is a dimensionless relative observation time defined by $\tau \equiv [c(t - t_c) - D + R_c]/R_c$, where D is the distance of

the fireball to the observer, and t is the observation time measured by the distant observer. In formula (1), $\tilde{I}(\tau_\theta)$ represents the development of the intensity magnitude of radiation in the observer frame, called as a local pulse function, and $g_{0,\nu}(\nu_{0,\theta})$ describes the rest frame radiation mechanisms.

Light curves determined by equation (1) are dependent on the integral limits $\tilde{\tau}_{\theta,\min}$ and $\tilde{\tau}_{\theta,\max}$, which are determined by the concerned area of the fireball surface, together with the emission ranges of the radiated frequency and the local time. But for commonly adopted mechanisms, such as the bremsstrahlung, Comptonized and synchrotron radiations, they cover the entire frequency band, and do not provide constraints on the integral limits (see equations (14) and (15) in Qin 2002). Thus the integral limits are only determined by $\tilde{\tau}_{\theta,\min} = \max\{\tau_{\theta,\min}, (\tau - 1 + \cos \theta_{\max})/(1 - \beta \cos \theta_{\max})\}$ and $\tilde{\tau}_{\theta,\max} = \min\{\tau_{\theta,\max}, (\tau - 1 + \cos \theta_{\min})/(1 - \beta \cos \theta_{\min})\}$, where $\tau_{\theta,\min}$ and $\tau_{\theta,\max}$ are the lower and upper limit of τ_θ confining $\tilde{I}(\tau_\theta)$, and θ_{\min} and θ_{\max} are confined by the concerned area of the fireball surface. The radiations are observable within the range of $(1 - \cos \theta_{\min}) + (1 - \beta \cos \theta_{\min})\tau_{\theta,\min} \leq \tau \leq (1 - \cos \theta_{\max}) + (1 - \beta \cos \theta_{\max})\tau_{\theta,\max}$ (see Paper II).

Because peak times of different light curves associated with different frequency intervals $[\nu_1, \nu_2]$ or different energy bands $[E_1, E_2]$ are different, following Shen et al. (2005), we define the spectral lag as the time between the peaks of the light curves in two different channels, a lower energy channel $[E_1, E_2]$ and a higher energy channel $[E_3, E_4]$. In the following, we will investigate on what parameters the lags are dependent in terms of the fireball model.

For the sake of simplicity, we employ in the following a local Gaussian pulse and employ the Band function as a rest frame radiation spectrum which was frequently and rather successfully employed to fit the spectra of GRBs (see, e.g., Schaefer et al. 1994; Ford et al. 1995; Preece et al. 1998, 2000) to study the issue. A local Gaussian pulse and the Band function are written as

$$\tilde{I}(\tau_\theta) = I_0 \exp\left[-\left(\frac{\tau_\theta - \tau_{\theta,0}}{\sigma}\right)^2\right] \quad (\tau_{\theta,\min} \leq \tau_\theta), \quad (2)$$

and

$$g_{0,\nu}(\nu_{0,\theta}) = \begin{cases} \left(\frac{\nu_{0,\theta}}{\nu_{0,p}}\right)^{1+\alpha_0} \exp\left[-(2 + \alpha_0)\frac{\nu_{0,\theta}}{\nu_{0,p}}\right] & \left(\frac{\nu_{0,\theta}}{\nu_{0,p}} < \frac{\alpha_0 - \beta_0}{2 + \alpha_0}\right) \\ \left(\frac{\alpha_0 - \beta_0}{2 + \alpha_0}\right)^{\alpha_0 - \beta_0} \exp\left(\beta_0 - \alpha_0\right) \left(\frac{\nu_{0,\theta}}{\nu_{0,p}}\right)^{1+\beta_0} & \left(\frac{\nu_{0,\theta}}{\nu_{0,p}} \geq \frac{\alpha_0 - \beta_0}{2 + \alpha_0}\right) \end{cases}, \quad (3)$$

respectively, where I_0 , σ and $\tau_{\theta,\min}$ are constants, α_0 and β_0 are the low and high energy indices in the rest frame, respectively, and $\nu_{0,p}$ is the rest frame peak frequency. Typical

values of the low and high energy indices coming from statistical analysis are $\alpha_0 = -1$ and $\beta_0 = -2.25$, respectively (see Preece et al. 1998, 2000).

Due to the constraint to the lower limit of τ_θ , which is $\tau_{\theta,min} > -1/\beta$ (see Paper II), we assign $\tau_{\theta,0} = 10\sigma + \tau_{\theta,min}$ so that the interval between $\tau_{\theta,min}$ and $\tau_{\theta,0}$ would be large enough to make the rising phase of the local pulse close to that of the Gaussian pulse. From (2) one can obtain $\Delta\tau_{\theta,FWHM} = 2\sqrt{\ln 2}\sigma$, which leads to $\sigma = \Delta\tau_{\theta,FWHM}/2\sqrt{\ln 2}$, where $\Delta\tau_{\theta,FWHM}$ is the FWHM of the Gaussian pulse. From the relation between τ_θ and t_θ , one gets $\Delta t_{\theta,FWHM} = (R_c/c)\Delta\tau_{\theta,FWHM}$. In the following, we assign $(2\pi R_c^3 I_0)/(hcD^2) = 1$, $R_c = 3 \times 10^{15}$ cm, $\tau_{\theta,min} = 0$, $\theta_{min} = 0$, and $\theta_{max} = \pi/2$.

2.1 Lag's dependence on the Lorentz factor and the local pulse width

As shown in Qin et al. (2004), the Lorentz factor and the local pulse width are important in producing the light curve observed. We wonder if the Lorentz factor and the local pulse width play important roles in producing a lag. The spectral lag of GRBs could be found either in high BATSE energy channels or in lower Ginga ones (see, e.g., Cheng et al. 1995; Chen et al. 2005; Norris et al. 1996, 2000; Wu & Fenimore 2000). We consider the following three different energy channel pairs: BATSE channels 1 and 3, BATSE channels 1 and 4, and Ginga channels between 2-10 keV and 50-100 keV (marked as Lag_{13} , Lag_{14} and Lag_G , respectively).

As suggested by observation, the value of the peak energy E_p of the GRB's νF_ν spectrum is mainly distributed within $100 \sim 600$ keV (See Preece et al. 2000) and peaks at about 250 keV. Here we assume 250 keV and 50 keV as the typical values of the peak energy of hard and soft bursts, respectively. In addition, we assume that typical hard and soft bursts come from the same Lorentz factor of the expanding motion of the fireball surface and differ only in their rest frame peak energy $E_{0,p}$. As derived in Qin (2002), when taking into account the Doppler effect of fireballs, the observed peak energy would be related with the peak energy of the typical rest frame Band function spectrum ($\alpha_0 = -1$, $\beta_0 = -2.25$) by $E_p \simeq 1.67\Gamma E_{0,p}$. In a recent work, the Lorentz factors of a GRB sample were found to be distributed mainly within (100, 400) and to peak at about 200 (Qin et al. 2005a). So, when assigning $\Gamma = 200$ to be the Lorentz factor of these sources, one would find the typical values of the rest frame peak energy $E_{0,p}$ of hard and soft bursts are 0.75 keV and 0.15 keV respectively.

Presented in Figs. 1 and 2 are the relationships between the lag and the Lorentz factor Γ as well as between the lag and the local pulse width, $\Delta t_{\theta,FWHM}$.

We find from the left panel in Fig. 1 that each of the three kinds of lag has a peak value. The Lorentz factor corresponding to this peak value is denoted by Γ_p (where subscript “p” stands for “peak”). The lags increase with Γ when $\Gamma < \Gamma_p$; the contrary is observed when $\Gamma > \Gamma_p$. For $E_{0,p} = 0.75keV$, the lags decrease with the Lorentz factor in the law of $lag \propto \Gamma^{-\epsilon}$ with $\epsilon > 2$ for the three kinds of lag. The figure exhibits $Lag_G < Lag_{13} < Lag_{14}$ within the range of $\Gamma > 100$ (note that current GRB models suggest that the gamma-ray photons come from a relativistically expanding fireball surface with Lorentz factor $\Gamma > 100$, see Piran 2005). The result and that obtained by Shen et al. (2005) are identical (note that here we fix the local pulse width instead of the co-moving pulse width). One can check that, when the local pulse width is large enough, for a fixed rest frame peak energy the observed peak energy would increase with Γ following the law of $E_p = 1.67\Gamma E_{0,p}$ for the adopted Band function spectrum (as shown in Qin 2002). According to the law of $E_p = 1.67\Gamma E_{0,p}$, the lag will have a peak value when E_p shifting from a higher energy channel to a lower one, which could be observed in Fig. 1. Fig. 1 shows that the relationship between the lag and Γ would differ according to different rest frame peak energy $E_{0,p}$, which suggests that, in producing a lag, not only the Lorentz factor is important but also the rest frame peak energy plays a role.

Fig. 2 shows that the lag increases with the local pulse width following the law of $Lag \propto \Delta t_{\theta,FWHM}$, and it obeys the law of $Lag_G < Lag_{13} < Lag_{14}$, the same as that shown in Fig. 1. However, as suggested by Fig. 2, the dependence of the lag on the local pulse width is much obvious than that on the Lorentz factor Γ and the rest frame peak energy $E_{0,p}$ (see Fig. 1). In a recent work, Lu et al. (2005a) found that $FWHM \propto \Delta t_{\theta,FWHM}$ based on the same model (Qin 2002, Qin et al. 2004), where $FWHM$ is the full width at half-maximum of the GRB’s light curve. Thus one could come to $lag \propto FWHM$, which is in agreement with the observation that wider pulses were found to produce longer lags (see Norris et al. 1996, 2001, 2005).

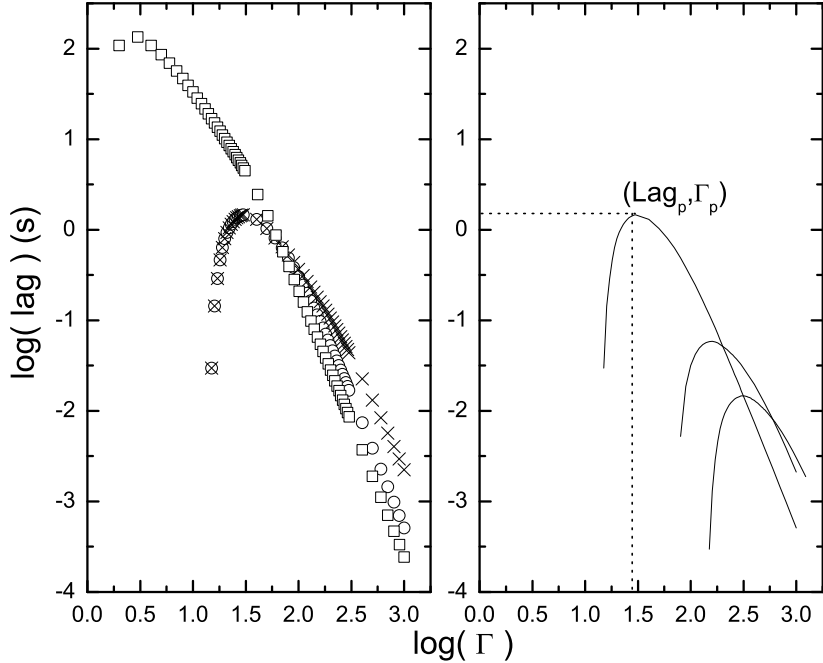


Figure 1. –Relationships between Lag_{13} , Lag_{14} , Lag_G and Γ for $E_{0,p}=0.75$ keV (the left panel), and that between Lag_{13} and Γ for different $E_{0,p}$ (the right panel), where the Band function rest frame radiation form with $\alpha_0 = -1$ and $\beta_0 = -2.25$ is adopted and we take $R_c = 3 \times 10^{15}$ cm and $\Delta t_{\theta,FWHM} = 10^5$ s. The open circle, the cross and the open square in the left panel stand for Lag_{13} , Lag_{14} and Lag_G , respectively. In the right panel, solid lines from the top to the bottom stand for $E_{0,p}=0.75$, 0.15, 0.075 keV, respectively.

2.2 Lag's dependence on spectral parameters of the Band function

We know that different values of the spectral parameters (i.e., α_0 , β_0 and $E_{0,p}$) of the Band function are associated with different mechanisms (see Band et al. 1993). Let us study the impact of the mechanisms on the spectral lag in the following.

We first investigate the lag's dependence on the observed peak energy of the νF_ν spectrum. Ignoring the minute difference caused by various factors, we assume that the following relationship holds in any situations concerned in this paper: $E_p = 1.67\Gamma E_{0,p}$ (one can check that, for photons emitted from an ejecta moving towards the observer, $E_p = 2\Gamma E_{0,p}$). This relationship tells us that the observed peak energy is proportional to Γ or $E_{0,p}$ when the other is fixed. The lag's dependence on the observed peak energy in the case of E_p varying with Γ when fixing $E_{0,p}$ is similar to those discussed in §2.1. For the sake of comparison, we convert the right panel of Fig. 1 to the last panel of Fig. 3 by applying the relationship. In addition, we explore the lag's dependence on the observed peak energy in the case of E_p varying with $E_{0,p}$ when fixing Γ .

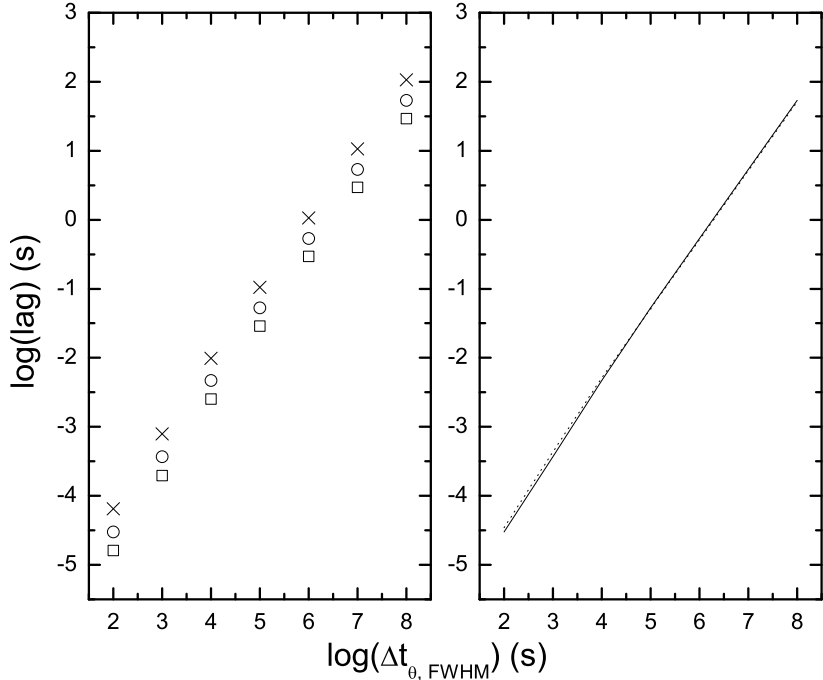


Figure 2. –Relationships between Lag_{13} , Lag_{14} , Lag_C and the local pulse width for $E_{0,p}=0.75$ keV (the left panel), and that between Lag_{13} and local pulse width (the right panel) for $E_{0,p}=0.75$ keV (the solid line) and 0.15 keV (the dotted line). Here we take $\Gamma = 200$. Other parameters and symbols are the same as those adopted in Fig. 1.

One would find from the left panel of Fig. 3 that, similar to Fig. 1, when E_p varies with $E_{0,p}$ for a fixed Γ , each of the three kinds of lag has a peak lag (Lag_p) as well.

To make clear what causes the relationships shown in Fig. 3, we divide the light curves of equation (1) into two parts, with one being contributed from the low-energy portion of the rest frame Band function spectrum and the other from the high-energy portion, and explore how the peak times, t_p , of the light curves are affected by the observed peak energy E_p when it shifting through the channel (see Figs. 4 and 5).

Let us denote the channel concerned by $[E_1, E_2]$ (for the first channel of BATSE, it is $[E_1, E_2] = [25, 50]$ keV, while for the third channel, it is $[E_1, E_2] = [100, 300]$ keV). From Figs. 4 and 5 some conclusions could be reached. For a certain value of the Lorentz factor (here we take $\Gamma = 100$), when $E_p < E_1$, the contributions to the light curves mainly come from the rest frame high-energy portion. According to the Doppler effect, this amount of energy would mainly come from the area of the fireball surface around the line of sight, i.e., $\theta \approx 0$ (where θ is the angle to the line of sight). In other words, energy arising from the rest frame high-energy portion (photons with $E_0 > E_{0,p}$ when emitted) emitted from the

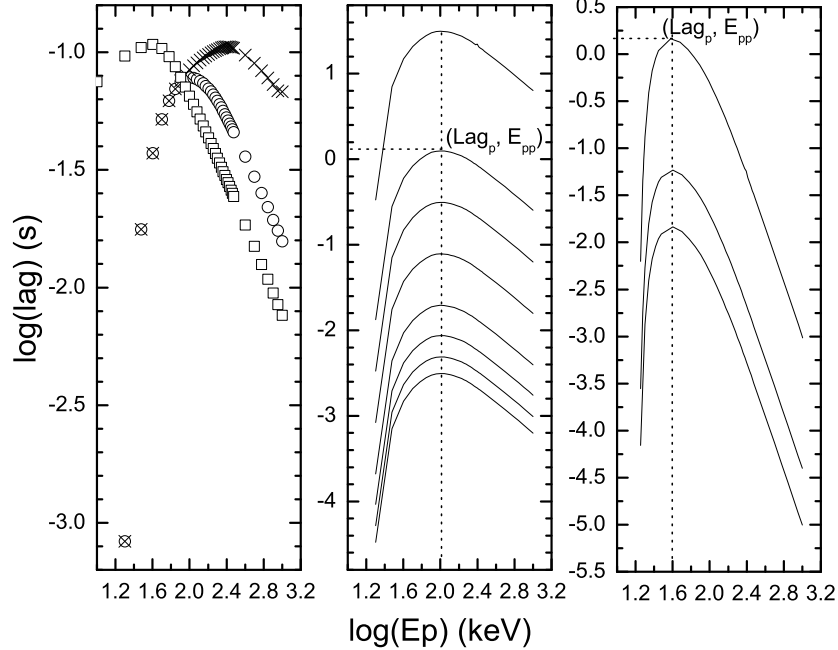


Figure 3. –Relationships between Lag_{13} , Lag_{14} , Lag_G and E_p for $\Gamma = 200$ (the left panel), and that between Lag_{13} and E_p for the two cases of fixing Γ (the middle panel) and $E_{0,p}$ (the last panel). In the middle panel, the solid lines from the top to the bottom represent $\Gamma=10, 50, 100, 200, 400, 600, 800, 1000$, respectively, and in last panel, the solid lines from the top to the bottom stand for $E_{0,p}=0.75, 0.15, 0.075$ keV, respectively. Other parameters and symbols are the same as those adopted in Fig. 1.

area with $\theta \approx 0$ would shift into the channel concerned, and thus the peak time t_p of the corresponding light curves would keep almost unchanged (see Fig. 5). When E_p increases, the contributions to the light curves from the low-energy portion become larger since the corresponding photons begin to shift into the channel concerned. At the same time, some high energy photons emitted from the area corresponding to a larger θ fall into the channel as well, and due to the well-known time delay their contributions to the observed light curves cause a larger t_p (see Fig. 5). It is the difference of t_p of two different channels that leads to a lag (see Fig. 1). When $E_{0,p}$ is fixed, the situation is quite different. In this case, the enhancement of E_p comes from the increasing of Γ . A large E_p corresponds to a large Γ which makes the light curve narrower (i.e., $FWHM \propto \Gamma^{-2}$, see Qin et al. 2004; Lu et al. 2005a). As a result, t_p sharply decreases with E_p (see the upper panels of Fig. 4 and the right panel of Fig. 5). Note that, since the influence of the Lorentz factor is very significant (as $FWHM \propto \Gamma^{-2}$), the difference of t_p of two different channels is hardly detectable in the right panel of Fig. 5.

Figs. 6 and 7 show that the lag increases with the low energy spectral index α_0 of the

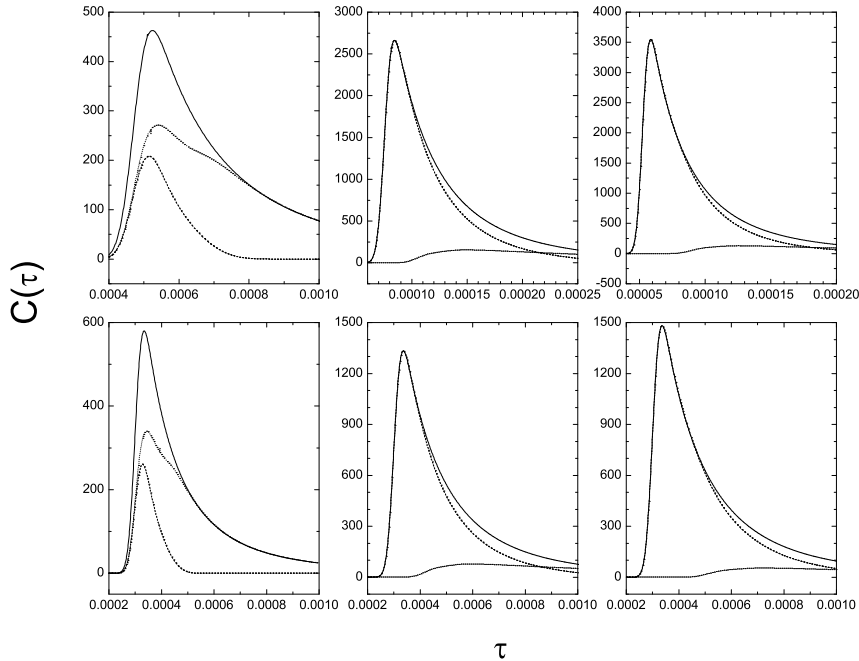


Figure 4. –Plots of the light curves of BATSE channel 3 contributed from the rest frame low-energy portion (the dash line) and high-energy portion (the dot line), and from the whole energy range (the solid line) of a Band function spectrum in cases of fixing $E_{0,p} = 0.75\text{keV}$ (the upper panels) and $\Gamma = 100$ (the lower panels). The panels from the left to the right stand for $E_p=100\text{ keV}$, 250 keV , 300 keV , respectively. Other parameters are the same as those adopted in Fig. 1.

rest frame Band spectrum and it decreases with the high energy spectral index β_0 of the spectrum. The relationships also follow $Lag_G < Lag_{13} < Lag_{14}$ in both cases. Compared with that associated with the low energy spectral index, the variation of the lag with respect to the increase of β_0 is relatively mild, where Lag_{13} and Lag_G are almost unchanged (see Fig. 7).

To investigate what causes the relationships shown in Figs. 6 and 7, once more we divide the light curves of equation (1) into two parts, as done in Fig. 4, here different α_0 and β_0 are adopted (see Figs. 8 and 9).

Fig. 8 shows that, for BATSE channel 3 and in the case of $E_p = 250\text{keV}$, when β_0 is fixed, the contribution from the rest frame low-energy portion to the light curve decreases slightly with the increasing of α_0 , whereas the contribution from the rest frame high-energy portion slightly increases with the increasing of α_0 . The peak time t_p of the first channel light curve of BATSE rises more rapidly than that of the third channel (see Fig. 8). Note that, to shift into the channel observed, photons of the rest frame high-energy portion must be those emitted from the area of larger θ , and it must be this that leads to the increasing

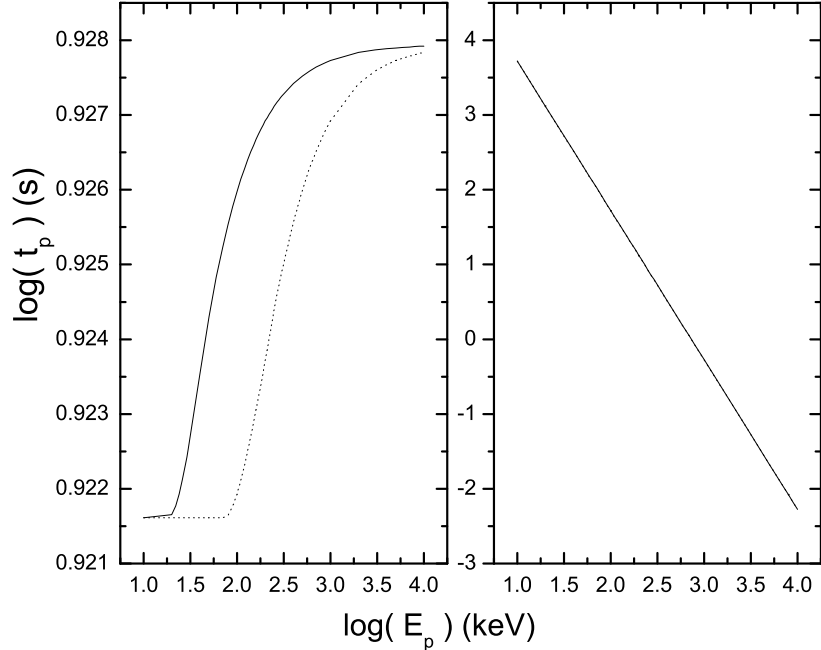


Figure 5. –Relationships between E_p and the peak time t_p of the light curves of BATSE channels 1 and 3 in cases of fixing $\Gamma = 200$ (the left panel) and $E_{0,p} = 0.75\text{keV}$ (the right panel). Here we take $R_c - D - ct_c = 0$. Other parameters are the same as those adopted in Fig. 4. The solid and the dot line stand for BATSE channels 1 and 3, respectively. (Note that the two lines in the right panel almost overlap each other.)

of t_p with the increase of α_0 . The difference of t_p of the two channel light curves causes the lag (see Fig. 6).

From Fig. 9 we find a slightly different situation. For BATSE channel 3 and in the case of $E_p = 250\text{keV}$, when α_0 is fixed, the contribution from the rest frame high-energy portion to the light curve is significant only when β_0 is close to -2 . The peak time t_p of the first channel light curve is almost unchanged with the increase of β_0 . Only when E_p is low enough, the contribution from the rest frame high-energy portion to the light curve could become significant. In this situation, the peak time t_p of the third channel would rise with the increase of β_0 (see Fig. 9). This is because that when E_p is low photons of the rest frame high-energy portion emitted from the area of larger θ would shift into the channel observed, and then the index β_0 would play a role.

2.3 Spectral lag in the case of a rest frame spectrum varying with time

It is common that the spectrum parameters of many GRBs are observed to vary with time (see Preece et al. 2000). We are curious how the lag's dependence on Γ and $\Delta t_{\theta,FWHM}$

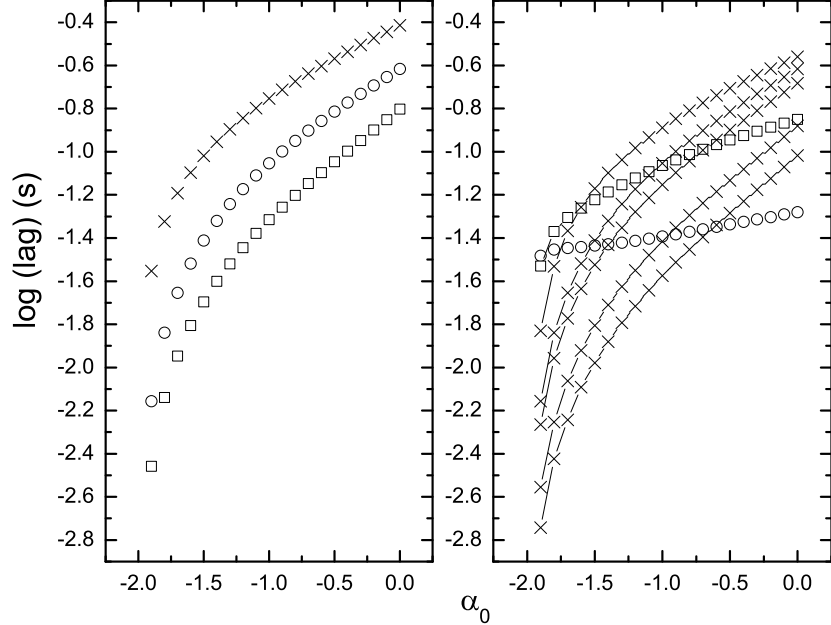


Figure 6. –Relationships between Lag_{13} , Lag_{14} , Lag_G and α_0 for $E_{0,p}=0.75$ keV (the left panel), and that between Lag_{13} and α_0 for different $E_{0,p}$ (the right panel). Here we take $\beta_0 = -2.25$ and $\Gamma = 200$. In the right panel, the open circle and the open square represent $E_{0,p} = 0.1\text{keV}, 0.15\text{keV}$, respectively, crosses from the top to the bottom represent $E_{0,p} = 0.35\text{keV}, 0.75\text{keV}, 1\text{keV}, 2\text{keV}, 3\text{keV}$, respectively. Other parameters and symbols are the same as those adopted in Fig. 1.

would be if the rest frame spectrum develops with time. As most of GRBs show “hard-to-soft” evolutionary feature (see e.g., Ford et al. 1995; Fishman et al. 1995; Band, David L. 1997; Preece et al. 1998;), here we consider a simple case where the rest frame spectrum is a Band function with its indices and the peak energy $E_{0,p}$ decreasing with time. Like Qin et al. (2005b), we assume a simple evolution of indices α_0 and β_0 and peak energy $E_{0,p}$ which follow $\alpha_0 = -0.5 - k(\tau_\theta - \tau_{\theta,1})/(\tau_{\theta,2} - \tau_{\theta,1})$, $\beta_0 = -2 - k(\tau_\theta - \tau_{\theta,1})/(\tau_{\theta,2} - \tau_{\theta,1})$ and $\log\nu_{0p} = 0.1 - k(\tau_\theta - \tau_{\theta,1})/(\tau_{\theta,2} - \tau_{\theta,1})$ (keVh^{-1}) for $\tau_{\theta,1} \leq \tau_\theta \leq \tau_{\theta,2}$. For $\tau_\theta < \tau_{\theta,1}$, $\alpha_0 = -0.5$, $\beta_0 = -2$ and $\log\nu_{0p} = 0.1$ (keVh^{-1}), while for $\tau_\theta > \tau_{\theta,2}$, $\alpha_0 = -0.5 - k$, $\beta_0 = -2 - k$ and $\log\nu_{0p} = 0.1 - k$ (keVh^{-1}). We take $k=0.1, 0.5$ respectively (they correspond to different rates of decreasing) to investigate the lag’s dependence.

Let us employ local Gaussian pulse (2) to study this issue. We adopt $\tau_{\theta,1} = 9\sigma + \tau_{\theta,min}$ and $\tau_{\theta,2} = 11\sigma + \tau_{\theta,min}$ and $\tau_{\theta,0} = 10\sigma + \tau_{\theta,min}$ and $\tau_{\theta,min} = 0$.

Figs. 10 and 11 show the dependence of lag on the Lorentz factor and the local pulse width in the case when parameters of the rest frame spectrum vary with time. We find that, when the spectral parameters decrease with time, the lags are larger than that associated

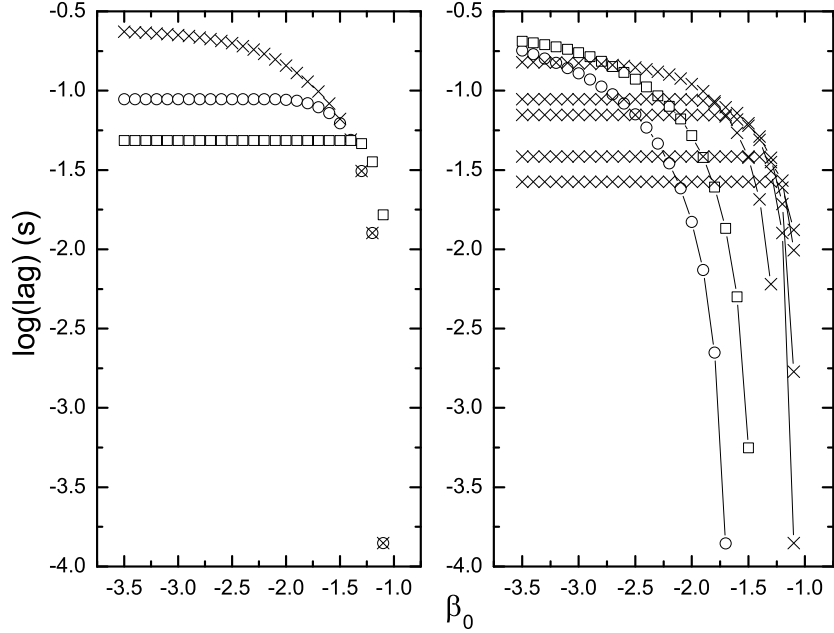


Figure 7. –Relationships between Lag_{13} , Lag_{14} , Lag_G and β_0 for $E_{0,p}=0.75$ keV (the left panel), and that between Lag_{13} and β_0 for different $E_{0,p}$ (the right panel). Here we take $\alpha_0 = -1$ and $\Gamma = 200$. Other parameters and symbols are the same as those adopted in Fig. 6.

with the case when the spectral parameters are fixed. The larger the decreasing speed (say, $k=0.5$), the more obvious the effect.

Kocevski et al. (2003a) argued that the observed lag is the direct result of spectral evolution and found the observed lag increases with the peak energy's decay rate. Motivating by this, we take $\alpha_0 = -0.5$, $\beta_0 = -2$, and allow E_{0p} varying with time. Illustrated in Fig. 12 is the relationship between the Lag_{13} and the rest frame peak energy decaying rate, k , which is in agreement with the observed result found by Kocevski et al. (2003a). The dependence of lag on the varying speed k in the case of the rest frame spectrum parameters α_0 and β_0 varying with time is also shown in Fig. 12. We find it common that the lag increases with the increasing of k . The increasing of lag in the case when the rest frame peak energy decreasing with time is much more obvious than that in the case when indexes α_0 and β_0 decreasing with time.

2.4 Lag's dependence on energy

In a previous study, Wu & Fenimore (2000) detected no larger lags in lower energy bands. However, we find from the above analysis that the following relation holds in almost all the

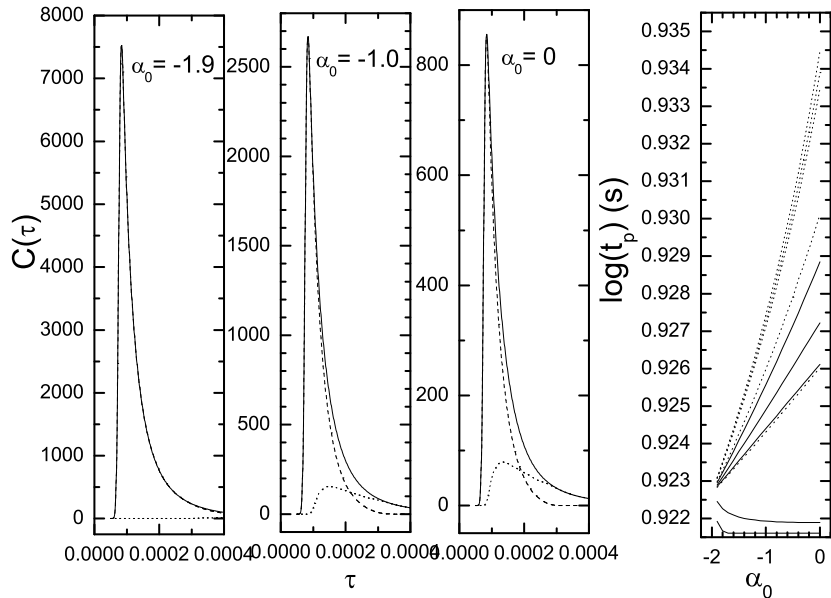


Figure 8. –Plots of the light curves of BATSE channel 3 contributed from different portions of the rest frame Band function spectrum for $E_p = 250\text{keV}$ (the first three panels) and the relationship between the peak time of the light curves of BATSE channel 3 (the solid lines) and 1 (the dot lines) and α_0 for different E_p (the last panel). Here we take $\beta_0 = -2.25$ and $\Gamma = 200$. In the first three panels, the dot, dash and solid lines represent the light curves contributed from the high-energy portion, the low-energy portion and the whole energy range of the adopted spectra, respectively. The solid lines (or the dot lines) from the bottom to the top in the last panel stand for $E_p = 50, 100, 250, 300, 400$ keV, respectively. The Other parameters are the same as those adopted in Fig. 5.

cases concerned: $Lag_G < Lag_{13} < Lag_{14}$. Motivated by this, we investigate in the following in much detailed the time lag's dependence on energy. We adopt a typical Band function spectrum with $\alpha_0 = -1$, $\beta_0 = -2.25$ and $E_{0,p} = 0.75\text{keV}$ as the rest frame radiation form to study this issue.

There are three instruments in the Swift telescope payload, and two of them could detect high energy photons with the XRT ranging from 0.2 keV to 10 keV and the BAT ranging from 15 keV to 150 keV (http://heasarc.gsfc.nasa.gov/docs/swift/about_swift/). We consider a wide band ranging from 0.2 keV to 8000 keV which covers both the Swift and BATSE bands. This band is divided into the following uniformly ranging channels (where $E_2 = 2E_1$): $[E_1, E_2] = [0.2, 0.4]$ keV, $[0.5, 1]$ keV, $[1, 2]$ keV, $[2, 4]$ keV, $[5, 10]$ keV, $[10, 20]$ keV, $[20, 40]$ keV, $[50, 100]$ keV, $[100, 200]$ keV, $[200, 400]$ keV, $[500, 1000]$ keV, $[1000, 2000]$ keV, $[2000, 4000]$ keV and $[4000, 8000]$ keV.

We measure the lags between the first channel and any of the other channels. The relationship between the lag and the corresponding energy E (here E denotes the lower energy limit of the corresponding high-energy channel) is presented in Fig. 13. It shows

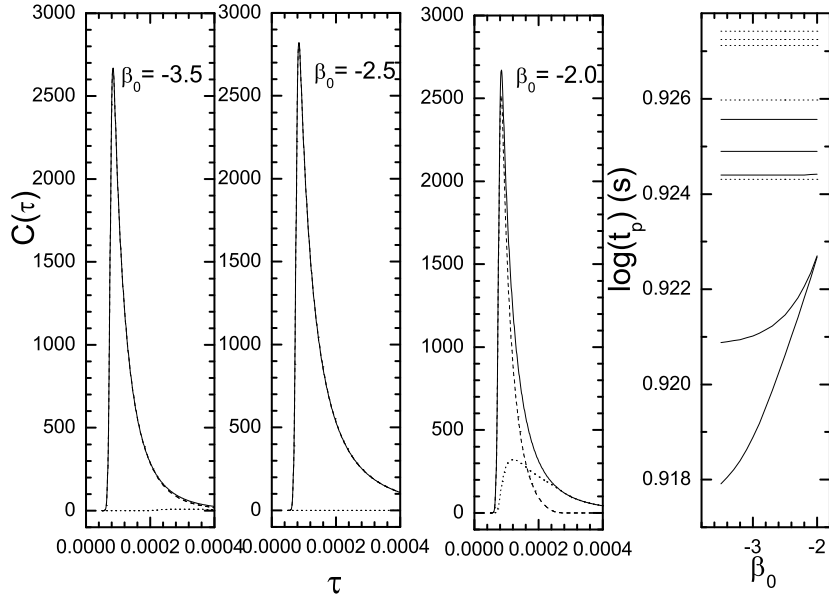


Figure 9. –Plots of the light curves of BATSE channel 3 contributed from different portions of the rest frame Band function spectrum for $E_p = 250\text{keV}$ (the first three panels) and the relationship between the peak time of the light curves of the light curves of BATSE channel 3 (the solid lines) and 1 (the dot lines) and β_0 for different E_p (the last panel). Here we take $\alpha_0 = -1$. Other parameters and symbols are the same as those adopted in Fig. 8.

that, for any given value of Γ , the lags increase with energy following the law of $lag \propto E$ and then saturate at a certain energy (we call E_s , where subscript “s” represents the word “saturate”). This might explain why Wu & Fenimore (2000) found that GRBs do not show larger lag at lower energy. We notice that E_s takes place behind the corresponding peak energy E_p (where the relation $E_p = 1.67\Gamma E_{0,p}$ is adopted). For different Γ , E_s increases with E_p following the law of $E_s \propto E_p$ (see the right panel of Fig. 13), and the relation $E_s \propto E_p$ holds for all $E_{0,p}$.

As shown in §2.2, when $E > E_p$, the contributions to the corresponding light curve largely come from the high-energy portion of the rest frame spectrum, which makes the peak time of the light curve less change, and thus the lag would saturate. The contrary is true. When $E \ll E_p$, the contributions come only from the low-energy portion of the rest frame spectrum, emitted from the whole fireball surface, i.e., $0 \leq \theta \leq \pi/2$. Thus, there would be almost no lag between the light curves of such two energy channels (see the two filled circles in the bottom of the left panel of Fig 13).

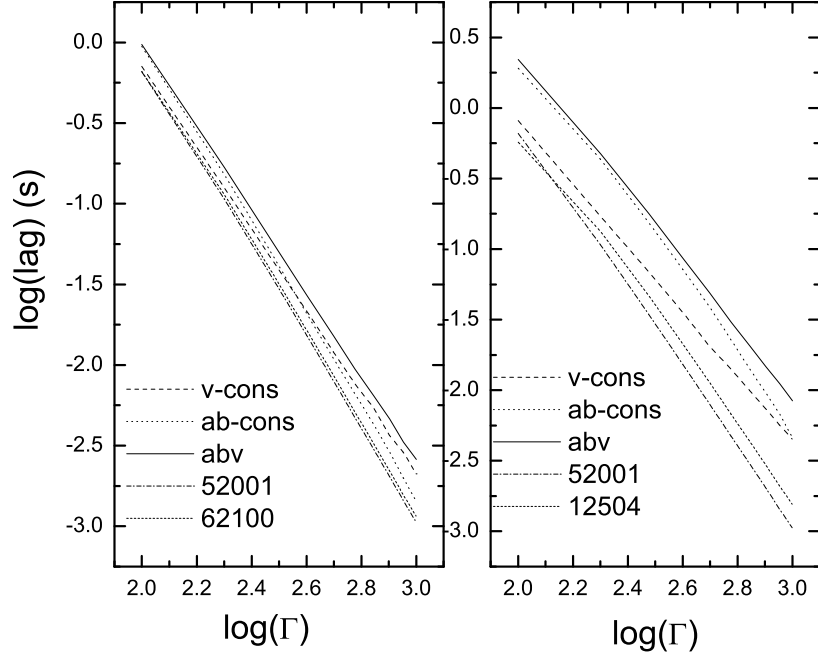


Figure 10. –Relationship between Lag_{13} and Γ associated with the situation when the rest frame spectrum varying with time in the case of $k = 0.1$ (the left panel) and $k = 0.5$ (the right panel). For the sake of comparison, the relationship deduced from the constant rest frame spectrum with the corresponding upper and lower limits of the indexes are also presented. The implications of the lines are as follows: v-cons (α_0 and β_0 varying with time, $\log\nu_{0p} = 0.1 \text{ keV}h^{-1}$); ab-cons ($\alpha_0 = -0.5$ and $\beta_0 = -2.0$, ν_{0p} varying with time); abv (α_0 , β_0 and ν_{0p} varying with time); 52001 ($\alpha_0 = -0.5$, $\beta_0 = -2.0$ and $\log\nu_{0p} = 0.1 \text{ keV}h^{-1}$); 62100 ($\alpha_0 = -0.6$, $\beta_0 = -2.1$ and $\log\nu_{0p} = 0.0 \text{ keV}h^{-1}$); 12504 ($\alpha_0 = -1.0$, $\beta_0 = -2.5$ and $\log\nu_{0p} = -0.4 \text{ keV}h^{-1}$). Here we take $\Delta t_{\theta,FWHM} = 10^5 \text{ s}$. Other parameters are the same as those adopted in Fig. 1.

2.5 Lag's dependence on the opening angle of uniform jets

According to the relativistic fireball model, emissions from a spherically expanding shell and a jet would be rather similar to each other as long as we are along the jet's axis and the Lorentz factor Γ of the relativistic motion satisfies $\Gamma^{-1} < \theta_j$, because the matter does not have enough time (in its own rest frame) to expand sideways at such a situation (Piran 1995, 1999). Let us study the dependence of lag on the radiated area confined by the opening angle of $\theta_{max} = p/\Gamma$, where p is a parameter describing the width of the opening angle of uniform jets. Shown in Fig. 14 is the relationship between Lag_{13} and p .

We find from Fig. 14 that Lag_{13} increases with the opening angle within $\theta_{max} < 0.6\Gamma^{-1}$ following the law of $Lag_{13} \propto p^{5.9}$, and beyond this range, it slightly increases with the angle, and finally saturates at $p = 0.8$ for any Γ . The saturate lag (denoted by Lag_s) decreases with the increasing of Γ following the law of $Lag_s \propto \Gamma^{-2.8}$ (see the right panel of Fig. 14). This is an outcome of the beaming effect. It suggests that there is a limited value of the lag

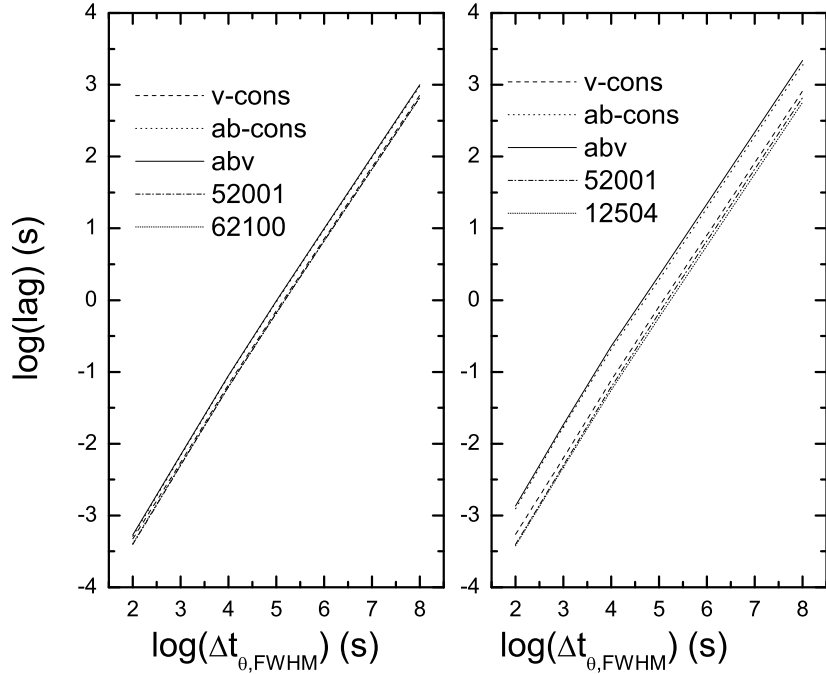


Figure 11. –Relationship between Lag_{13} and the local pulse width $\Delta t_{\theta,FWHM}$ associated with the situation when the rest frame spectrum varying with time in the case of $k = 0.1$ (the left panel) and $k = 0.5$ (the right panel). For the sake of comparison, the relationship deduced from the constant rest frame spectrum with the corresponding upper and lower limits of the indexes are also presented. Implications of the lines are the same as those in Fig. 10. Here we take $\Gamma = 100$. Other parameters are the same as those adopted in Fig. 1.

when different opening angles of uniform jets are concerned, which is the same as that in the case of spherical fireballs.

2.6 Lag's dependence on the radius of fireball

Shen et al. (2005) found that the lag is independent of the radius of fireballs based on their model (see Fig. 8 in their paper). We perform the analysis with their formula when raising a higher precision of calculation (the result is the same when we adopt equation [1]). Here we fix the local pulse width by adopting $\Delta t_\theta = 10s$. The result is presented in Fig. 15.

Fig. 15 shows that Lag_{13} decreases with the radius of fireballs following the law of $Lag_{13} \propto R_c^{-0.1}$, when the local pulse width is fixed. The lag depends on the radius of fireballs. Comparing our result with that obtained in Shen et al. (2005) we find that the conclusions are entirely different. We suspect that three factors might be responsible to this difference. The first is the precision of calculation. The second is the range concerned. Our calculation spans about three magnitudes of the fireball radius while Shen et al. (2005) considered only two magnitudes. The third is that the dependence of Lag_{13} on the radius is weak: the lag

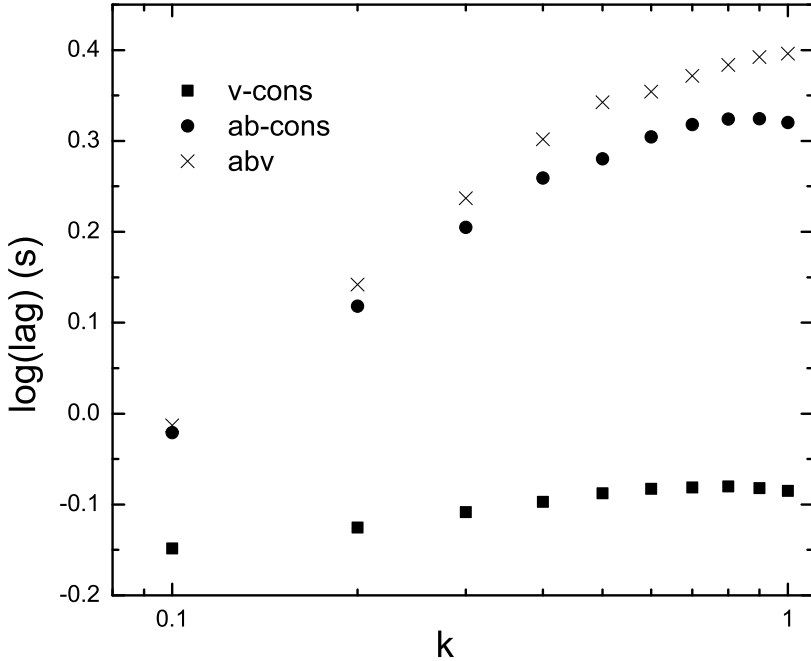


Figure 12. –Relationship between Lag_{13} and the varying speed k of the parameters of the rest frame spectrum. The implications of the lines are as follows: v-cons (α_0 and β_0 varying with time, $\log E_{0p} = 0.1 \text{ keV} h^{-1}$); ab-cons ($\alpha_0 = -0.5$ and $\beta_0 = -2$, E_{0p} varying with time); abv (α_0 , β_0 and ν_{0p} varying with time). Here we take $\Gamma = 200$ and $\Delta t_{\theta,FWHM} = 10^5 \text{ s}$. Other parameters are the same as those adopted in Fig. 1.

would be only about two times smaller when the radius becomes three magnitudes larger. We believe that the third is the key factor accounting for the difference.

The conclusion of Shen et al. (2005) that the lag is independent of the radius of fireballs is a puzzle since a large radius seems to cause a larger distance between the area with $\theta = 0$ and that with $\theta > 0$ on the fireball surface and this should lead to a larger lag. Our conclusion that the lag decrease slightly with the increasing of the radius makes the puzzle worse. The mechanism accounting for this is currently unclear. We suspect that this dependence might rely on what kind of photons dominate the peaks of the lower and higher energy channels respectively and where they are emitted from. In creating the dependence, other parameters such as the rest frame peak energy and the Lorentz factor might be at work. Therefore, this might not be answerable if only a simple mechanism is concerned (to find a answer to this, a detailed investigation should be made, which is beyond the scope of this paper).

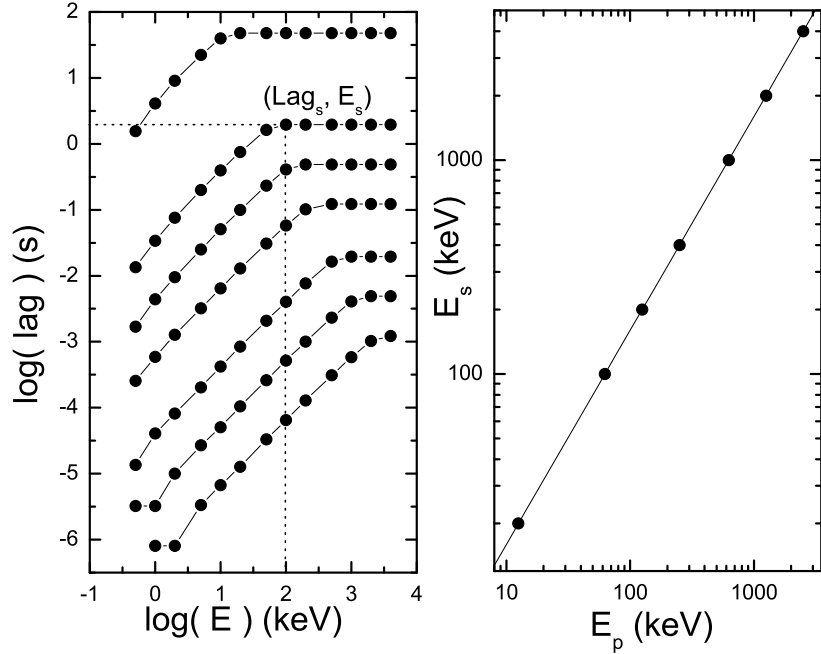


Figure 13. –Relationship between the lag and the lower energy limit E of the corresponding high energy channel for different Γ (the left panel) and that between E_s and E_p (the right panel), where the relationship $E_p = 1.67\Gamma E_{0,p}$ is adopted and we take $\alpha_0 = -1$, $\beta_0 = -2.25$ and $E_{0,p} = 0.75\text{keV}$. Solid lines from the top to the bottom in the left panel stand for $\Gamma=10, 50, 100, 200, 500, 1000, 2000$, respectively. The solid line in the right panel is the linear fit one of the data. Other parameters are the same as those adopted in Fig. 1.

3 DIFFERENT CHARACTERISTICS SHOWN IN THE TWO CASES OF FIXING THE INTRINSIC PULSE WIDTH AND THE LOCAL PULSE WIDTH

Shen et al. (2005) explored the lag's dependence on the Lorentz factor and found $\text{Lag} \propto \Gamma^{-1}$ when fixing the intrinsic pulse width (the co-moving pulse width) and the fireball radius. However, in this paper we find $\text{Lag} \propto \Gamma^{-2}$ instead, when fixing the local pulse width and the fireball radius based on both models of Shen et al. (2005) and Qin et al. (2004). According to the theory of special relativity, the two results are identical, as the local timescale is Γ times of the corresponding intrinsic timescale. Some interesting questions arise accordingly. When the fireball radius is fixed (as considered in Shen et al. 2005 and in this paper), would the two approaches always lead to identical results? Could they reveal the same property of the curvature effect? In which case should which one be preferred?

As pointed out and illustrated in Qin et al. (2004), the profiles of light curves are not affected by the Lorentz factor when fixing the relative local pulse width ($c\Delta t_\theta/R_c$, or $\Delta\tau_\theta$ as

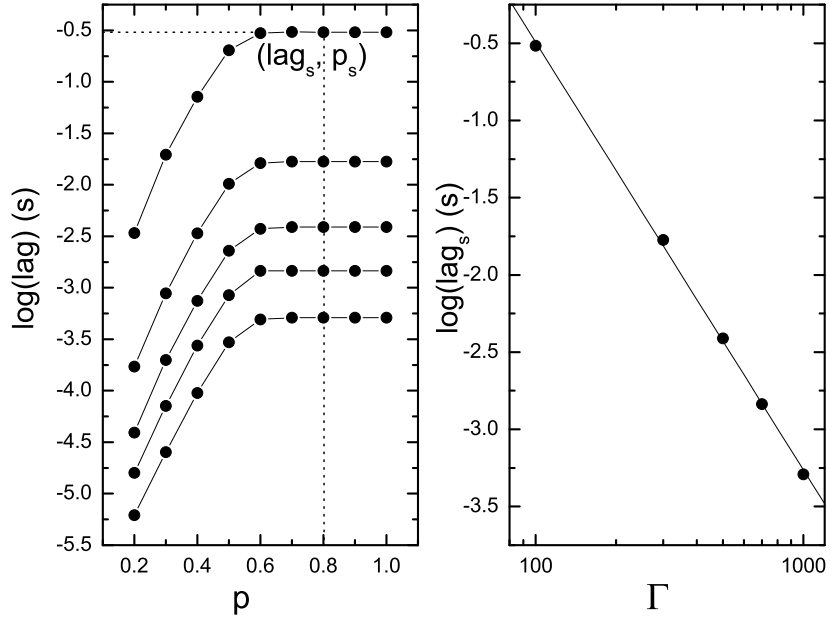


Figure 14. –Relationship between Lag_{13} and p for different Γ (the left panel), and that between lag_s and Γ (the right panel), where we adopt a typical Band function spectrum with $\alpha_0 = -1$, $\beta_0 = -2.25$ and $E_{0,p} = 0.75\text{keV}$ as the rest frame radiation form. In left panel, solid lines from the top to the bottom stand for $\Gamma = 100, 300, 500, 700, 1000$, respectively. Other parameters are the same as those adopted in Fig. 1.

used in Qin et al. 2004). When the fireball radius is fixed, a fixed relative local pulse width would correspond to a fixed local pulse width (that is, a certain $\Delta\tau_\theta$ leads to a certain Δt_θ in this situation, where R_c is fixed). Thus, in this situation, fixing the local pulse width would not lead to different profiles of light curves when different Lorentz factors are considered. However, the feature of the profile will change when fixing only the intrinsic pulse width. This is because that for a certain intrinsic pulse width, the corresponding local pulse width would take different values when different Lorentz factors are considered (recall that the local timescale is Γ times of the corresponding intrinsic timescale), and this would lead to different relative local pulse width since R_c is fixed. The corresponding profiles of light curves would change since they are sensitive to the relative local pulse width (see Qin et al. 2004).

Fig. 16 illustrates the different influences of the Lorentz factor on the profiles of the light curves calculated with equation (5) in Shen et al. (2005) in the two cases of fixing the local pulse width and the intrinsic pulse width.

Kocevski et al. (2003b) and Ryde et al. (2003) found that there is a linear relationship between the rise width, $FWHM_r$ and the full width, $FWHM$, of gamma-ray pulses. Lu et al. (2005a) explained the relationship based on the formula presented in Qin et al. (2004),

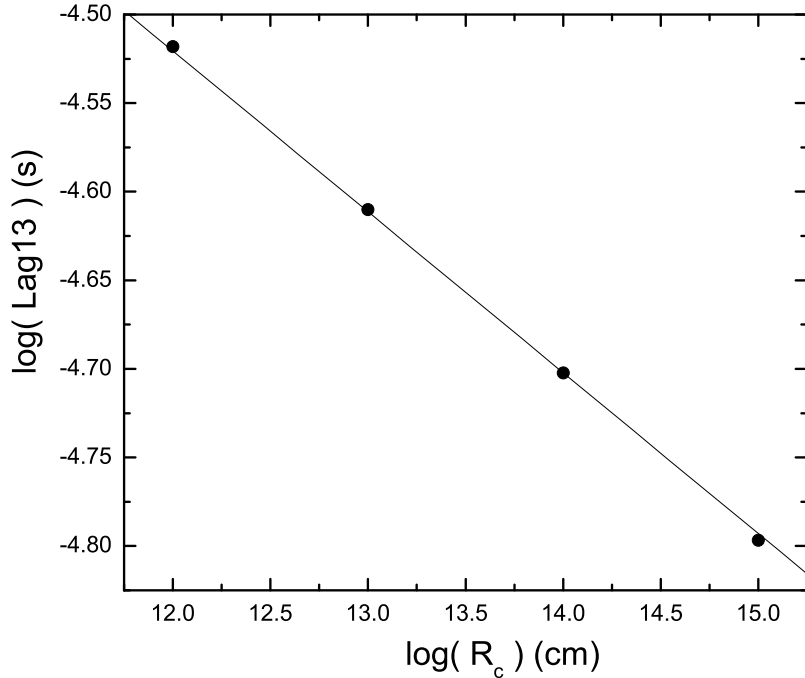


Figure 15. –Relationship between Lag_{13} and the radius of the fireball. Here we take $\Gamma = 100$, $E_{0,p} = 0.75\text{keV}$ and $\Delta t_{\theta,FWHM} = 10\text{s}$. The solid line is a linear fit to the data. Other parameters are the same as those adopted in Fig. 1.

and found that there exists a dead line in the $FWHM_r - FWHM$ plane when taking the relative local pulse width $\Delta\tau_{\theta,FWHM} \geq 1$. Here we repeat the same work as illustrated in Fig. 2 of Lu et al. (2005a) based on the Shen et al. (2005) formula. As shown in Fig. 17, we find that there indeed exists the dead line predicted before in the $FWHM_r - FWHM$ plane when fixing the local pulse width (here we take $td \geq 1000\text{s}$ and $R_c = 3 \times 10^{13}\text{cm}$ which corresponds to $\Delta\tau_{\theta,FWHM} \geq 1$). However, when fixing the intrinsic pulse width, one cannot find a dead line in the plane (see Fig. 17). This indicates that the features in the $FWHM_r - FWHM$ plane are different in the case of fixing the local pulse width and in that fixing the intrinsic pulse width. One could obtain the local pulse width td by measuring the location of the corresponding data (to observe in what lines they belong to) from the left panel of Fig. 17 as long as $\Delta\tau_{\theta,FWHM} < 1$. But one could not measure the intrinsic pulse width from the right panel of the figure. This indicates that the former is superior to the latter when one attempts to make use of the $FWHM_r - FWHM$ plane.

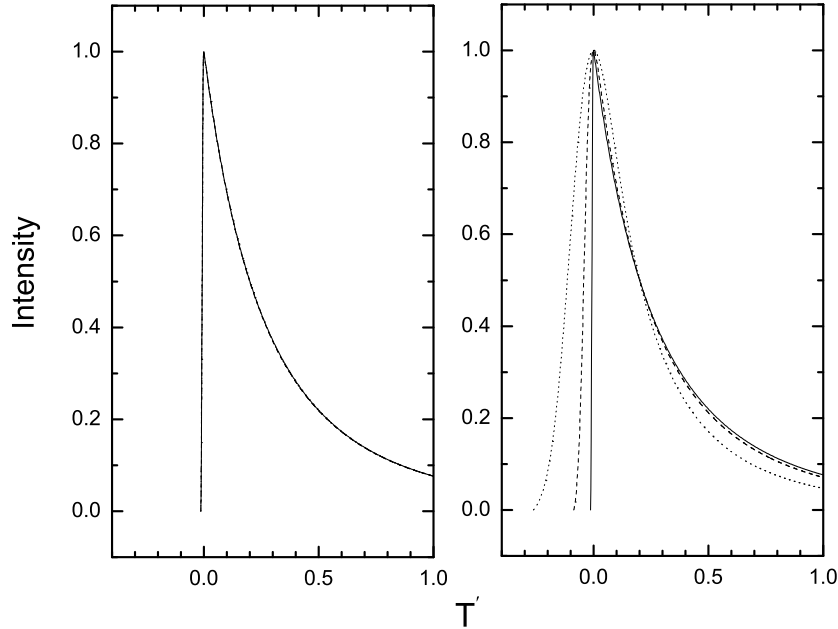


Figure 16. –Plots of the light curves of BATSE channel 3 resulting from symmetric Gaussian pulses when fixing the local pulse width $td = 100s$ (the left panel) and the intrinsic pulse width $td' = 10s$ (the right panel) for different Γ . Here we take $\alpha = -1$, $\beta = -2.25$, $R_c = 5 \times 10^{14} cm$ and $E_p = 350 keV$ (where the relationship $E_p = 1.67\Gamma E_{0,p}$ is adopted). The solid, dash and dot lines stand for $\Gamma = 10, 100, 1000$ respectively (the three lines in the left panel overlap each other). Note that, for the sake of comparison, we normalize the light curves and re-scale the variable so that the peak count rate is located at $T' = 0$ and the FWHM of the decay portion is located at $T' = 0.2$.

4 DISCUSSION AND CONCLUSIONS

Discussed in Shen et al. (2005) and the above analysis, only intrinsic or local Gaussian pulses are involved. One might ask if the conclusions hold only in the selected pulse form. Thus, we replace the local Gaussian pulse with other forms of local pulses when applying equation (1) and the corresponding formula of Shen et al. (2005). Local pulses (55), (81), (82), (83), (85), (86) and (87) presented in Qin et al. (2004) are studied. We find that the lags resulting from a local pulse without a decaying phase are too small to be noticed. For example, $lag_{13t} < 10^{-6}s$ when $\Gamma > 100$ and $R_c = 3 \times 10^{15} cm$. This is in well agreement with what discovered by Shen et al. (2005). Now it is clear that, in the mechanism of the curvature effect, it is the decaying phase of a local pulse that contributes to the observed lags.

A recent study revealed that (see Lu et al. 2005b), the rise phase of light curves will always be dominated by the emission from $\theta \simeq 0$ and within the rise phase of the local pulse. It is illustrated in Fig. 18, where a local pulse without a decaying phase is considered.

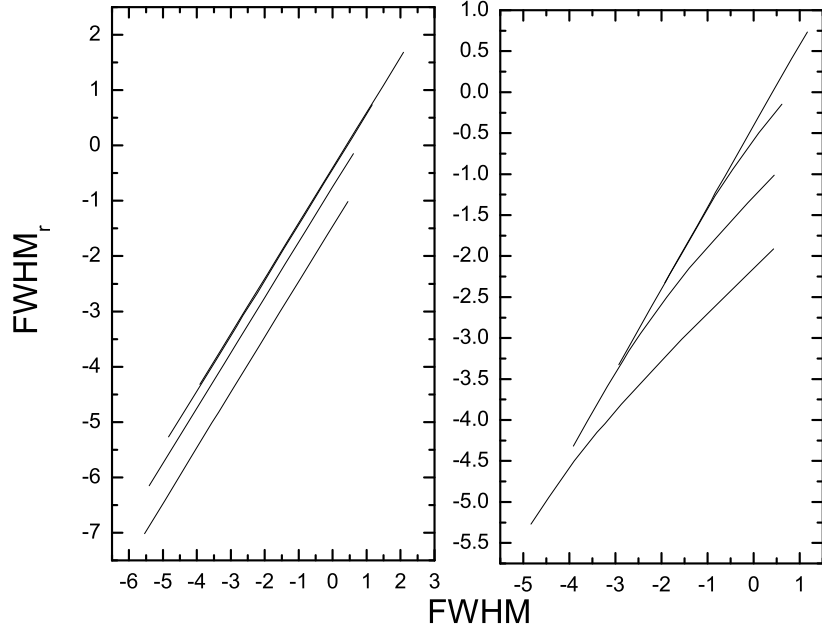


Figure 17. Relationships between $FWHM_r$ and $FWHM$ for the light curves of BATSE channel 3 resulting from symmetric Gaussian pulses associated with the case of fixing the local pulse width (the left panel) and the case of fixing the intrinsic pulse width (the right panel). In the left panel, solid lines from the bottom to the top represent $td = 10s, 100s, 1000s, 10000s$, respectively (note that the last two solid lines overlap each other), and in the right panel, the corresponding lines stand for $td' = 0.1s, 1s, 10s, 100s$, respectively. Here we take $R_c = 3 \times 10^{13} cm$ and other parameters are the same as those adopted in Fig. 16.

This indicates that there would be no peak lags for the light curves of different energy channels associated with those local pulses without a decaying phase.

Except the Band function spectrum, the Comptonized spectrum and the broken power law spectrum were employed to fit the spectral data in Preece et al. (2000). To make sure if the dependence of lags discussed above would be altered when other rest frame spectra are considered, we employ the Comptonized spectral model as the rest frame radiation form to investigate the lag's dependence concerned above. The Comptonized spectrum is written as $I_\nu \propto \nu_{0,\theta}^{1+\alpha_{0,C}} \exp(-\frac{\nu_{0,\theta}}{\nu_{0,C}})$, where $\alpha_{0,C}$ and $\nu_{0,C}$ are constants. Here, typical values, $\alpha_{0,C} = -0.6$ (Schaefer et al. 1994) and $\nu_{0,C} = 0.55 keV h^{-1}$ (see Qin 2002 Table 2) are adopted. Our calculation shows that the characteristics of the lag's dependence are the same as what revealed above, when the rest frame Band function spectrum is replaced with the two other forms. The only difference is the magnitude of the lags. For example, when the rest frame Comptonized spectral model is adopted, we obtain a slightly larger value of Lag_{13} (about 70% larger) when we redraw Fig. 2.

Of the sample of 41 source presented in Friedman et al. (2005), we find that the range of

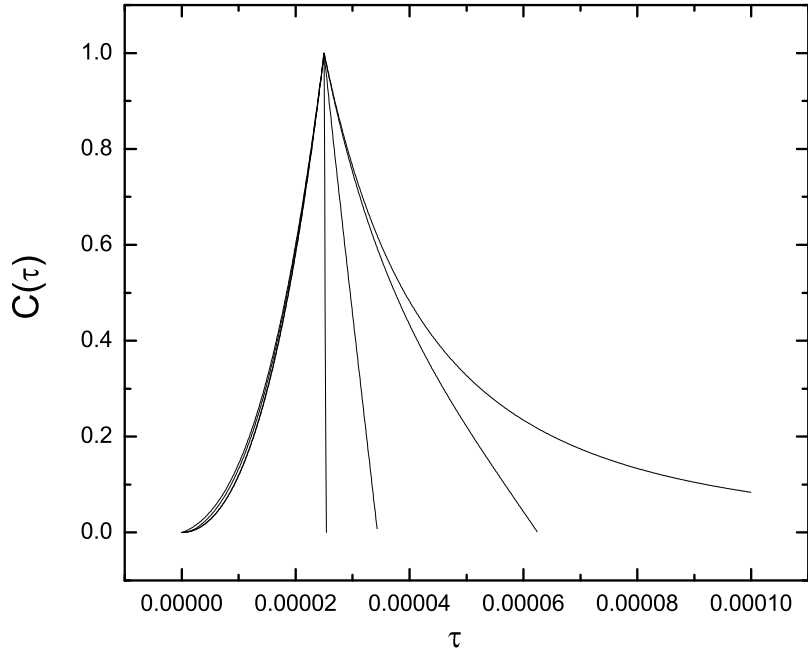


Figure 18. Plots of the normalized light curves of BATSE channel 3 arising from a local linear rise pulse with $\Delta\tau_{\theta,FWHM} = 1$ (a local pulse without a decaying phase) emitted from different areas of the fireball surface. Here we take $\Gamma = 200$ and adopt a Band function rest frame radiation form with $\alpha_0 = -1$, $\beta_0 = -2.25$ and $\nu_{0p} = 0.75\text{keV}\text{h}^{-1}$. The solid lines from the right to the left stand for $\theta_{max} = \pi/2$, $1/\Gamma$, $0.5/\Gamma$ and $0.1/\Gamma$, respectively (note that the rising phase as well as the peak of the counts rates for different light curves overlap each other). Other parameters are the same as those adopted in Fig. 1.

θ_j is $\{0.03107, 0.57072\}$ rad, and its average value is 0.15925 rad. It shows that $\theta_j \gg \Gamma^{-1}$ if $\Gamma > 100$. As discussed in §2.5, one could find that for GRBs coming from a uniform jet with such opening angles, if $\Gamma > 100$ is adopted, the difference of lags from that arising from a spherical surface would not be distinguishable.

Several authors showed that the CCF lags between BATSE channels 1 and 3 tend to concentrate near $< 200\text{ms}$ (see Norris et al. 1996, 2000; Chen et al. 2005). A recent measurement carried by Norris et al. (2005) for BATSE wide pulses showed that the long lag range is $1.0 < lag < 4.2$ s. It is generally believed that the gamma-rays arise from internal shocks at a distance of $R \sim 10^{13} - 10^{15}$ cm from the initial source (Piran 2005). Within the generally accepted ranges of $R_c = 10^{13} - 10^{15}$ cm and $\Gamma > 100$, the observed lags could be accounted for by the curvature effect when different values of parameters are adopted. For example, one gets $Lag_{13} = 300$ ms from Fig. 1 when taking $\Gamma = 100$; $Lag_{13} = 100\text{ms}$ from Fig. 7 when taking $\alpha_0 = -1$, $\beta_0 = -2.25$ and $E_{0,p} = 0.75\text{keV}$. According to Fig. 2, $Lag_{13} \simeq 4.6 \times 10^{-7} \Delta t_{\theta,FWHM}$ s. One could obtain a large lag, i.e., $Lag_{13} = 4.6$ s when

taking $\Delta t_{\theta,FWHM} = 10^7 s$. In this situation, the $FWHM$ of the corresponding light curve determined by equation (1) is about 75 s when taking $\Gamma = 500$, which is very close to the observed data of the wide-pulse bursts studied in Norris et al. (2005), i.e., $1.0 < lag < 4.2$ s and $6s < \text{the width of channel 1} < 100s$ (see Fig. 6 in that paper). All these show that merely the curvature effect could produce the observed lags. A larger lag requires a wider local pulse.

We thus come to the following conclusions: a) $lag \propto \Gamma^{-\epsilon}$ with $\epsilon > 2$ within different energy channels, and the relationship would be different for different rest frame peak energy E_{0p} ; b) lag is proportional to the local pulse width and the $FWHM$ of the observed light curves, and the local pulse width plays a more important role in producing a large lag when compared with other lag's dependent parameters; c) a large lag requires a large α_0 and a small β_0 as well as a large E_{0p} ; d) when the rest frame spectrum varies with time, the lag would become larger; e) lag decreases with the increasing of R_c ; f) $lag \propto E$ within a certain energy range for a given Γ ; g) lag is proportional to the opening angle of uniform jets when $\theta_{max} < 0.6\Gamma^{-1}$.

We are very grateful to Dr. Rong-feng Shen for sending us his valuable program and for his helpful suggestions. This work is supported by the Special Funds for Major State Basic Research Projects (“973”) and National Natural Science Foundation of China (No. 10273019 and No. 10463001).

REFERENCES

Band, D., Matteson, J., Ford, L., Schaefer, B., Palmer, D., Teegarden, B., Cline, T., Briggs, M., et al. 1993, *ApJ*, 413, 281

Band, David L. 1997, *ApJ*, 486, 928B

Chen, Li, Lou, Yu-Qing, Wu, Mei, Qu, Jin-Lu, Jia, Shu-Mei, Yang, Xue-Juan. 2005, *ApJ*, 619, 983

Cheng L. X., Ma Y.Q., Cheng K. S., Lu T. & Zhou Y. Y. 1995, *A&A*, 300, 746

Fishman, G., Meegan, C. 1995, *ARA&A*, 33, 415

Ford, L. A., Band, D. L., Matteson, J. L., Briggs, M. S., Pendleton, G. N., Preece, R. D., Paciesas, W. S., Teegarden, B. J., et al. 1995, *ApJ*, 439, 307F

Friedman, Andrew S. & Bloom, Joshua S. 2005, *ApJ*, 627, 1F

Ioka K. & Nakamura T. 2001, *ApJ*, L163

Kocevski D. & Liang E. 2003a, *ApJ*, 594, 385

Kocevski D., Ryde F., & Liang E., 2003b, *ApJ*, 596, 389

Lu, R. J., Qin, Y. P., & Yi, T. F., 2005a, *Chin. J. Astron. Astrophys.*, in press, astro-ph/0508599

Lu, R. J., Qin, Y. P., 2005b, *MNRAS*, Submitted, astro-ph/0508537

Norris, J. P., Nemiroff, R. J., Bonnell, J. T., Scargle, J. D., Kouveliotou, C., Paciesas, W. S., Meegan, C. A., Fishman, G. J. 1996, *ApJ*, 459, 393

Norris, J. P., Marani G. F., & Bonnell J. T. 2000, *ApJ*, 534, 248

Norris J. P., Scargle, J. D. & Bonnell, J. T. 2001, astro-ph/0105052

Norris, J. P., Bonnell, J. T., Kazanas, D., Scargle, J. D., Hakkila, J., Giblin, T. W. 2005, *ApJ*, 627, 324N

Piran, T. 1995, in *AIP Conf. Proc. 307, Gamma-Ray Bursts: Second Huntsville Workshop*, ed. G. J. Fishman, J. J. Brainerd, & K. Hurley (New York: AIP), 495

Piran, T. 1999, *Phys. Rep.*, 314, 575

Piran, T. 2005, *Rev. Mod. Phys.* 76, 1143

Preece, R. D., Pendleton, G. N., Briggs, M. S., Mallozzi, Robert S., Paciesas, William S., Band, David L., Matteson, James L., Meegan, C. A. 1998, *ApJ*, 496, 849

Preece, R. D., Briggs, M. S., Mallozzi, R. S., Pendleton, G. N., Paciesas, W. S. and Band, D. L. 2000, *ApJS*, 126, 19

Qin, Y.-P. 2002, *A&A*, 396, 705

Qin, Y.-P. 2003, *A&A*, 407, 393

Qin, Y. P., Zhang Z. B., Zhang F. W. and Cui X. H. 2004, *ApJ*, 617, 439 (Paper II)

Qin, Y.-P., & Zhang, B.-B. 2005a, astro-ph/0504070

Qin, Y.-P., & Dong, Y.-M., & Lu R.-J., B.-B. Zhang, L.-W. Jia 2005b, *ApJ*, 632, 1008

Ryde F., Borgonovo L., Larsson S. et al., 2003, *A&A*, 411, L331

Schaefer, Bradley E., Teegarden, Bonnard J., Fantasia, Stephan F., Palmer, David, Cline, Thomas L., Matteson, James L., Band, David L., Ford, Lyle A., et al. 1994, *ApJS*, 92, 285S

Schaefer, Bradley E. 2004, *ApJ*, 602, 306

R.-F. Shen, L.-M. Song, Z. Li, 2005, *MNRAS*, 362, 59S (Paper I)

Salmonson J. D. 2000, *ApJ*, 544, L115

Wu B. & Fenimore E. 2000, *ApJ*, 535, L29